PROTON TESTING

EMCORE MTX8501/MRX8501
(12 x 1.25 Gbps Parallel Array Transmitter and Receiver Modules)

Crocker Nuclear Laboratory
U.C. Davis.
1st February, 2002

P. Marshall, M. Carts, S. Buchner
NASA/GSFC
Greenbelt MD 20771

1. Introduction

The MTX8501 and MRX8501 are 12 channel, high-speed transmitter and receiver modules for use in parallel optical data communication links. The modules perform logic-to-light and light-to-logic conversions for data transmission over multimode fiber ribbon cable, at a wavelength of 850 nm. Each of the 12 channels can transmit at a maximum of 1.25 Gbps, giving a maximum data transmission rate of 15 Gbps.

The transmitter consists of an array of vertical cavity surface emitting lasers (VCSELs) that generate the light for data transmission through the fiber cables. The data sheet does not mention the type of detector, but it is most likely a PIN photodiode optimized for light detection at 850 nm, a product listed in EMCORE's product line.

Both modules were subjected to radiation testing by exposing them to a beam of 63 MeV protons to determine their sensitivity to both single-event effects (SEEs) and to total dose damage, including both total ionizing dose (TID) and displacement damage dose. (With the actual transmitter and receiver devices being located inside a metal housing, testing with heavy ions could not be done.)

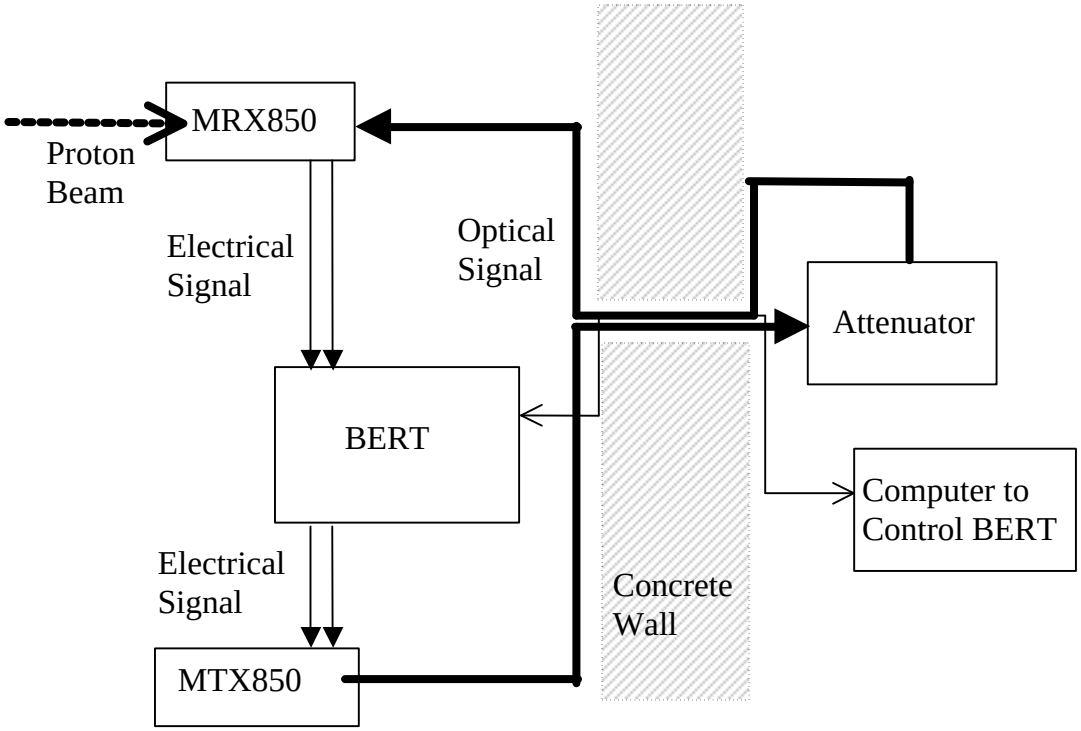

Fig. 1. Diagram showing setup during proton testing.

2. Test Conditions

Proton testing was carried out at Crocker Nuclear Laboratory using 63 MeV protons to determine the SEE and TID/DD response of the transmitter and receivers.

Both the transmitter and receiver were mounted on individual evaluation boards that minimize stray capacitances and allow for maximum frequency operation. The boards are:

- Transmitter on TX, 1.25 Gbps Test Board 600864 Rev 4
- Receiver on RX, 1.25 Gbps Test Board 600863 Rev 4

Two SMA connectors are required for each channel because the electrical input signals are in the form of differential voltages. The power supply to the board was 5 V, but 3.3 V was derived on the board for powering the parts. Fig. 1 shows the setup used for testing. The electrical input signal was supplied by the Bit Error Rate Tester (BERT). 62/125 MM FO cables were connected to the output of the transmitter and the input of the detector via MO connectors. An attenuator was inserted in the optical path to reduce the light intensity in order to measure the optical power budget, i.e., how much spare light intensity was available above the point at which there would be a significant increase in the bit error rate caused by noise in the system.

For proton testing, only one channel was used. The electrical signal consisted of a bit stream of logical “1s” and “0s” obtained from a pseudo-random number generator. The transmitter converted the electrical signal into an optical signal, which was transmitted through the optical fiber to a receiver, where it was converted back into an electrical signal. The signal from the detector was compared with that originally supplied to the emitter. Differences were flagged and noted as errors. Before exposing the device-under-test (DUT) to the proton beam, the light intensity arriving at the receiver was adjusted using the attenuator to determine the optical power budget.

In the actual setup, the transmitter and receiver were both located in the target room. The receiver was placed in front of the proton beam because previous experience suggests that the photo-detector, not the VCSEL, is the source of most SEEs. The optical cable from the transmitter in the target room was routed through a conduit in the concrete walls of the target chamber and connected to the attenuator located in the vicinity of the experimenters. The light intensity was measured using a light wave multimeter 8163A from Agilent. The output of the attenuator was routed back through the conduit to the receiver positioned in front of the beam. In this way it was possible to modify the attenuation without having to enter the target chamber.

Each test run involved a different set of experimental parameters, including angle, attenuation and transmission rate. The following are the reasons for varying this set of parameters: i) Detectors with large lateral dimensions are known to exhibit a marked increase in the bit error rate for protons near grazing incidence, i.e., near 90^{o}, due to single-event transients (SETs) caused by direct ionization, ii) the error rate increases with decreasing light intensity, and iii) the error rate increases with increasing data transmission rate.

To facilitate angular measurements, the board with the device-under-test was mounted on a stage with both translational and rotational degrees of freedom. The stage was used both to align the part and to change the angle of incidence.

The proton beam current was 5000 pA to ensure sufficient SETs for good statistics and for doing the test in a cost-effective manner. At the same time, there would not be too many either to

overwhelm the system or run the danger of multiple hits during the transmission of one bit of data. Table I shows the pertinent information about the boards and parts.

Table I. Identification numbers for evaluation boards, transmitter and receiver

Function	**Evaluation Board**	**Device Serial Number**
Transmitter	TX, 1.25GB/S 600864 Rev 4	A1 312-12
Receiver	RX, 1.25GB/S 600863 Rev 4	A1 233-01

3. Results

a. Single-Event Transients

Table II in the appendix shows a summary of the pertinent SET data obtained. Two different receivers (photodiodes) and one transmitter were tested. For testing of the transmitter, the receiver was removed from in front of the accelerator exit port and replaced by the transmitter. The data for the transmitter (Run #67) show that no SETs were generated when the transmitter was irradiated with protons.

The BER showed a significant increase when the proton beam was close to grazing incidence: at an angle of 90 degrees, the BER was more than an order of magnitude greater than at 20 degrees. The actual BER was found to depend on both the attenuation setting and the data transmission rates. This suggests that SETs in the detectors can be produced via direct ionization by protons traveling over the long paths lengths in the lateral direction of PIN diodes. Ionization from secondary particles produced through collisions between protons and atomic nuclei would not exhibit the enhancement at large angles of incidence. The noise floors at the different data transmission rates are listed in Table II in the appendix.

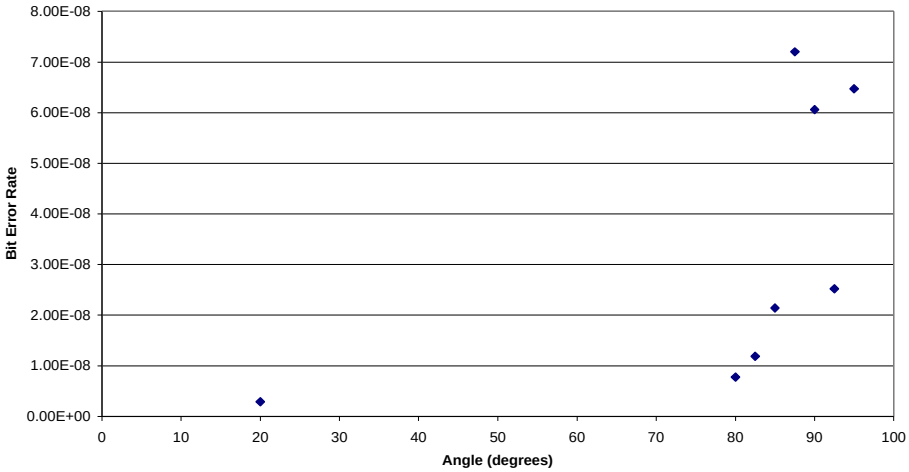

Fig. 2. Bit error rate as a function of proton beam angle of incidence for a data rate of 1.25 GHz, showing the significant increase at 90 degrees.

Figures 2 and 3 show that there an enhancement in the bit error rate when the angle of incidence is 90 degrees and the enhancement is greater at higher data rates.

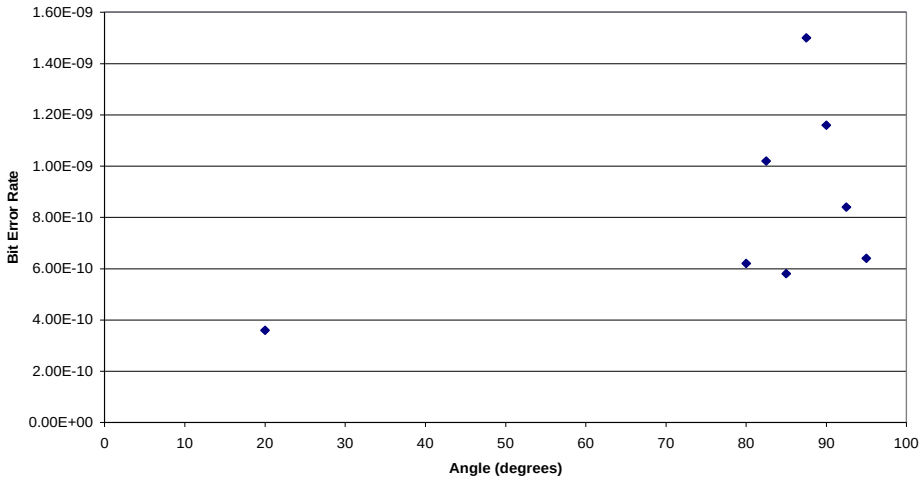

Fig. 3. Bit error rate as a function of angle of proton beam angle of incidence for a data rate of 125 MHz showing an approximately fourfold increase in the error rate at 90 degrees.

In all cases of high light intensity and low data rate, the number of errors equals the number of events, i.e., there are only single bit errors and no error bursts. However, in runs 40 → 42, and runs 52 → 60 the total number of bits in error exceeds the total number of events, suggesting that in those cases there were occasionally bursts of upsets. The bursts are consistent with the low signal intensity i.e., high attenuation, and high data rate.

Fig. 4 shows the BER as a function of attenuation setting for different transmission rates and at an angle of incidence of 20 degrees. It is evident that the BER increases with increasing attenuation and that the effect is more pronounced at higher data rates. Both of these effects are consistent with previous data on optical receivers.

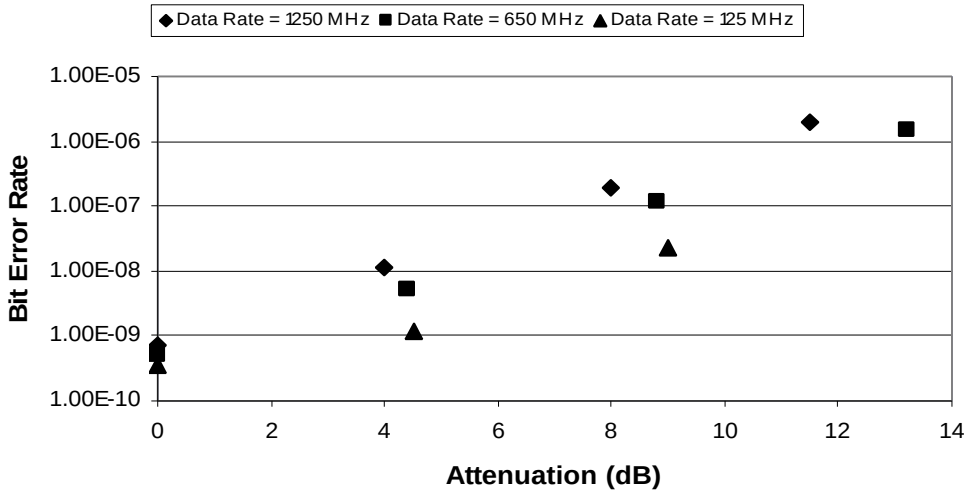

Fig. 4. Bit error rate as a function of attenuation for different transmission data rates at an incident angle of 20 degrees. Clearly, the bit error rate increases with increasing attenuation and, for fixed attenuation, with increasing frequency.

Fig. 5 shows the BER as a function of attenuation setting for different transmission rates for protons incident at 90 degrees. The same general behavior is noted, but the increase in BER as a function of attenuation setting is much less than for normal incidence.

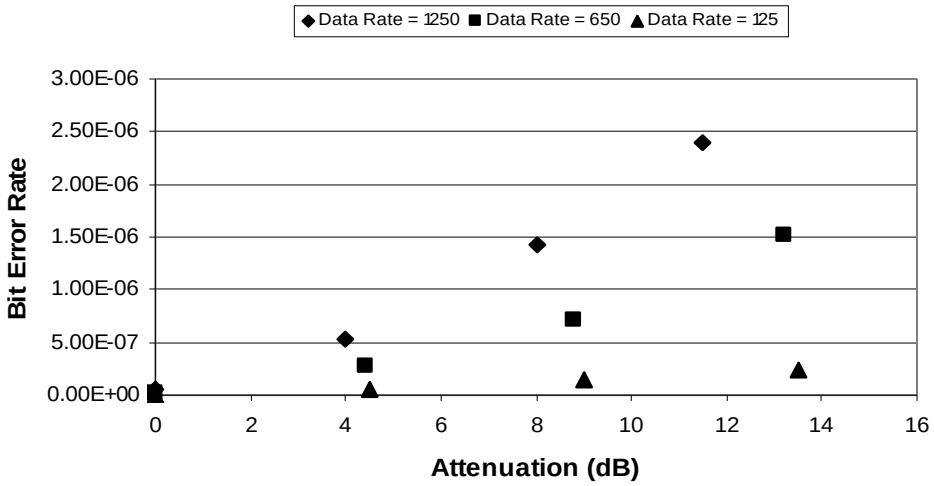

Fig. 5. Bit error rate as a function of attenuation for different data transmission rates and for an angle of incidence of 90 degrees.

b. Damage due to TID/DD

The first detector was exposed to a total fluence of 7.16×10^{11} protons/cm^2. This is equivalent to a TID of 103 krad(Si).

Following this exposure, there was no change in the functioning of the device, nor in the current supplied to the board. The second detector was exposed to a TID of 30.7 Krad(Si) from the 63 MeV protons and no change was observed. The transmitter was exposed to a fluence of 2×10^{11} protons/cm^2 which is equivalent to a TID of 28.8 Krad(Si) and no change in error rate or operating parameters was observed.

Table III shows the noise floor as a function of data rate, where the noise floor is the magnitude of the attenuation (in dB) required in order to obtain an error rate of 1.00E-12 per second.

Table IV shows the power available for each channel (in dBm). Only channel 1 (in both RX and TX) was used for these measurements so that the maximum power available was –5.3 dBm.

4. Conclusions

The EMCORE transmitter/receiver pair has been tested for proton induced SETs and damage in the form of TID/DD. The receiver is sensitive to proton induced SETs and the resulting bit error rates depend on angle of incidence, transmission rate and attenuation setting. The transmitter is not sensitive to SETs. The parts are also not sensitive to TID/DD up to levels of approximately 100 krad(Si).

Table II. Bit error rate cross sections for various angles, data rates and attenuations.

Run #	DUT	Atten.	Fluence	Angle	Data Rate	No. Errors	No. Events	Cross-section
1	MRX8501-1	0	1.00E+10	20	1250	25	25	2.50E-09
2	MRX8501-1	0	5.00E+10	20	1250	118	116	2.36E-09
3	MRX8501-1	0		20	650			
4	MRX8501-1	0	5.00E+10	20	650	59	59	1.18E-09
5	MRX8501-1	0	5.00E+10	20	125	18	18	3.60E-10
6	MRX8501-1	0	5.00E+10	80	125	31	31	6.20E-10
7	MRX8501-1	0	5.00E+10	82.5	125	51	51	1.02E-09
8	MRX8501-1	0	5.00E+10	85	125	29	29	5.80E-10
9	MRX8501-1	0	5.00E+10	87.5	125	75	75	1.50E-09
10	MRX8501-1	0	5.00E+10	90	125	58	58	1.16E-09
11	MRX8501-1	0	5.00E+10	92.5	125	42	42	8.40E-10
12	MRX8501-1	0	5.00E+10	95	125	32	32	6.40E-10
13	MRX8501-1	0	2.00E+10	95	1250	180	180	9.00E-09
14	MRX8501-1	0	1.00E+10	92.5	1250	180	180	1.80E-08
15	MRX8501-1	0	1.00E+10	90	1250	608	608	6.08E-08
16	MRX8501-1	0	1.00E+10	87.5	1250	647	647	6.47E-08
17	MRX8501-1	0	1.00E+10	92.5	1250	252	252	2.52E-08
18	MRX8501-1	0	1.00E+10	90	1250	606	606	6.06E-08
19	MRX8501-1	0	1.00E+10	87.5	1250	720	720	7.20E-08
20	MRX8501-1	0	1.00E+10	85	1250	214	214	2.14E-08
21	MRX8501-1	0	1.00E+10	82.5	1250	119	119	1.19E-08
22	MRX8501-1	0	1.00E+10	80	1250	78	78	7.80E-09
23	MRX8501-1	0	1.00E+10	20	1250	29	29	2.90E-09
24	MRX8501-1	0	1.00E+10	90	650	169	169	1.69E-08
25	MRX8501-1	0	1.00E+10	90	125	24	24	2.40E-09
26	MRX8501-1	4.5	1.00E+10	90	125	510	510	5.10E-08
27	MRX8501-1	4.4	5.00E+09	90	650	1360	1360	2.72E-07
28	MRX8501-1	4	1.00E+09	90	1250	525	525	5.25E-07
29	MRX8501-1	4	5.00E+09	20	1250	57	57	1.14E-08
30	MRX8501-1	4.4	5.00E+09	20	650	27	27	5.40E-09
31	MRX8501-1	4.5	1.00E+10	20	125	12	12	1.20E-09
32	MRX8501-1	9	5.00E+09	20	125	117	117	2.34E-08
33	MRX8501-1	8.8	1.00E+09	20	650	118	118	1.18E-07
34	MRX8501-1	8	1.00E+09	20	1250	194	194	1.94E-07
35	MRX8501-1	8	1.00E+09	90	1250	1431	1431	1.43E-06
36	MRX8501-1	8.8	1.00E+09	90	650	718	718	7.18E-07
37	MRX8501-1	9	1.00E+09	90	125	149	149	1.49E-07
38	MRX8501-1	13.5	1.00E+09	90	125	239	239	2.39E-07
39	MRX8501-1	13.2	1.00E+09	90	650	1516	1516	1.52E-06
40	MRX8501-1	11.5	1.00E+09	90	1250	2396	?	2.40E-06
41	MRX8501-1	11.5	1.00E+09	20	1250	1944	1941	1.94E-06
42	MRX8501-1	13.2	1.00E+09	20	650	1440	1438	1.44E-06
43	MRX8501-1	13.5	1.00E+09	20	125	283	283	2.83E-07
44	MRX8501-1	13.5	1.00E+09	80	125	469	469	4.69E-07
46	MRX8501-1	13.5	1.00E+09	82.5	125	454	454	4.54E-07
47	MRX8501-1	13.5	1.00E+09	85	125	373	373	3.73E-07
48	MRX8501-1	13.5	1.00E+09	87.5	125	330	330	3.30E-07
49	MRX8501-1	13.5	1.00E+09	90	125	275	275	2.75E-07
50	MRX8501-1	13.5	1.00E+09	92.5	125	335	335	3.35E-07
51	MRX8501-1	13.5	1.00E+09	95	125	399	399	3.99E-07

Run #	DUT	Atten.	Fluence	Angle	Data Rate	No. Errors	No. Events	Cross-Section
52	MRX8501-1	11.5	1.00E+09	95	1250	3483	3471	3.48E-06
53	MRX8501-1	11.5	1.00E+09	92.5	1250	2766	2753	2.77E-06
54	MRX8501-1	11.5	1.00E+09	90	1250	2314	2266	2.31E-06
55	MRX8501-1	11.5	1.00E+09	87.5	1250	2421	2374	2.42E-06
56	MRX8501-1	11.5	1.00E+09	85	1250	2814	2766	2.81E-06
57	MRX8501-1	11.5	1.00E+09	82.5	1250	3519	3500	3.52E-06
58	MRX8501-1	11.5	1.00E+09	80	1250	3836	3823	3.84E-06
59	MRX8501-4	11.9	1.00E+09	20	1250	1923	1922	1.92E-06
60	MRX8501-4	11.9	1.00E+09	90	1250	2276	2244	2.28E-06
61	MRX8501-4	0	1.00E+09	90	1250	42	42	4.20E-08
62	MRX8501-4	0	1.00E+10	20	1250	13	13	1.30E-09
63	MRX8501-4	0	5.00E+10	20	125	8	8	1.60E-10
64	MRX8501-4	0	5.00E+10	90	125	88	88	1.76E-09
65	MRX8501-4	14.3	5.00E+10	90	125	15245	15245	3.05E-07
66	MRX8501-4	14.2	5.00E+10	20	125	15829	15829	3.17E-07
67	MTX8501-4	8	2.00E+11	20	1250	0	0	0.00E+00

Table III. Noise floors for BER of 1E-12 for different frequencies and attenuation settings.

Data Rate (Gbps)	Noise Floor (dB) below 0 dB Attenuation	Actual Attenuation Settings Used (dB)
0.125	14.4	0, 4, 5, 9, 13.4
0.650	13.7	0, 4.4, 8.8, 13.2
1.25	12.2	0, 4, 8, 12

Table IV. Optical Power (dBm) in each channel.

Channel Number	Power (dBm)
1	-5.3
2	-12.9
3	-12.3
4	-8.3
5	-13.6
6	-4.9
7	-25.0
8	-4.5
9	-6.5
10	-8.6
11	-3.5
12	-15.7